MOLECULAR AND CELLULAR BIOLOGY, Nov. 1986, p. 4088–4092
0270-7306/86/114088-05$02.00/0
Copyright © 1986, American Society for Microbiology
Vol. 6, No. 11

NOTES

Deregulation of the c-*myc* Oncogene in Virus-Induced Thymic Lymphomas of AKR/J Mice

ALISE REICIN,[1] JIAN-QING YANG,[2] KENNETH B. MARCU,[2] ERWIN FLEISSNER,[1] CHARLES F. KOEHNE,[1] AND PAUL V. O'DONNELL[1]*

Program in Molecular Biology, Memorial Sloan-Kettering Cancer Center, New York, New York 10021,[1] and Department of Biochemistry, State University of New York at Stony Brook, Stony Brook, New York 11794[2]

Received 22 October 1985/Accepted 11 June 1986

A high frequency (≥65%) of thymomas induced by mink cell focus-forming virus 69L1 in AKR/J mice contain proviral integrations which are clustered 0.7-kilobase upstream of the c-*myc* oncogene predominantly in the opposite transcriptional orientation. Blot hybridization experiments showed that on the average there was only a twofold elevation of steady-state c-*myc* RNA in the thymomas as compared with levels in normal AKR/J thymocytes. Such an increase would not appear to be sufficient as a mechanism of oncogene activation in this system. In contrast, S1 nuclease analysis of transcripts initiated from the two known c-*myc* promoters indicated a strong shift in promoter usage in virtually all thymomas tested. In normal thymus the ratio of transcripts initiated from the proximal promoter P1 to the distal promoter P2 was 0.2 to 0.3. In contrast, most of the thymomas tested (18 of 23) showed an average P1/P2 ratio of 1.2 regardless of whether or not proviral integrations could be detected within a 21-kilobase *Eco*RI fragment containing the three c-*myc* exons. We conclude that alterations in P1/P2 ratios are good indicators of c-*myc* deregulation in thymic lymphomas.

The c-*myc* oncogene has been implicated in a variety of malignant neoplasms. In lymphoid tumors of both B- and T-cell lineages activation of c-*myc* has been associated with DNA rearrangements at the c-*myc* locus caused by either chromosomal translocations or retrovirus insertions (for a recent review, see reference 25). Recently, we reported murine leukemia virus proviral integrations into the c-*myc* locus in 65% of thymic lymphomas induced by intrathymic injection of mink cell focus-forming virus (MCF) 69L1 into 40-day-old AKR/J mice (13). In this report we measured steady-state levels of both total c-*myc* RNA and c-*myc* transcripts initiated from each of the two known promoters of the gene to study the effect of proviral integration on expression of the c-*myc* oncogene. We present evidence that expression of c-*myc* is not increased markedly in MCF-induced thymomas but is deregulated in tumors as evidenced by a reversal of normal promoter usage. Altered levels of the two c-*myc* transcripts also were observed in many instances in which a proviral integration was not detected near c-*myc*.

A map of MCF proviral integration sites for 40 independent primary thymomas which have been analyzed to date is shown in Fig. 1. Most (32 of 40) of the proviral integrations were in the reverse transcriptional orientation to c-*myc* and were distributed about a median distance 0.7-kilobase (kb) 5′ of exon 1, a finding similar to that reported by other workers (3, 9, 19). Of the eight tumors with colinear proviral integrations, only two of them, with insertions at +0.7 kb and +5.2 kb, were available for analysis in this study.

Steady-state levels of c-*myc* RNA were measured by slot-blot analysis of total cellular RNA (Fig. 2a). Samples of total RNA (2) in 4.6 M formaldehyde–7.5 × SSC (0.1 M sodium chloride, 0.01 M sodium citrate) were heated at 65°C for 15 min, diluted serially, and applied to two separate nitrocellulose filters by use of a slot-blotter manifold (Schleicher & Schuell, Inc., Keene, N.H.). Each sample well was washed with 400 μl of 10× SSC. All filters were baked at 80°C for 2 h. To detect c-*myc* RNA, one filter was prehybridized for 15 to 30 min at 42°C with 50% formamide, 5× SSC, 7 mM Tris hydrochloride (pH 7.4), 5× Denhardt solution, 100 μg of denatured salmon sperm DNA per ml, 0.2% sodium dodecyl sulfate, and 6% dextran sulfate. Filters were then hybridized with 2.0×10^7 cpm of ^{32}P-labeled nick-translated (16) probe B (Fig. 1) for 18 to 20 h at 42°C under stringent conditions. Filters were then washed twice at room temperature 2× SSC–0.1% sodium dodecyl sulfate, twice at 55°C with 2× SSC–0.1% sodium dodecyl sulfate, and once at 65°C with 0.1× SSC–0.1% sodium dodecyl sulfate. The total amount of poly(A)-containing RNA per sample was determined with a second filter which was prehybridized as described above. Filters were then rinsed twice with 0.1× SSC and hybridized for 2.5 h at 37°C in a mixture of 0.67× SSC, 1× Denhardt solution, 100 μg of salmon sperm DNA per ml, 200 μg of yeast tRNA per ml, 50 mM phosphate buffer, and 10 mM EDTA with 7 μg of cold poly(dT) per ml and 10^6 cpm of end-labeled (10) poly(dT) per ml. Filters were then washed twice with 0.67× SSC and 0.1× SSC at 42°C. After washing, all blots were exposed to Kodak XR-5 film in the presence of an intensifying screen at −70°C. Specificity controls included total yeast RNA which did not hybridize to the c-*myc* probe. Other controls not shown were yeast tRNA which did not hybridize to either c-*myc* or poly(dT) probes, RNase treatment of samples which eliminated both c-*myc* and poly(dT) signals, and Northern blot analysis of selected samples which showed only the expected c-*myc* signal at 2.2 to 2.4 kb.

Levels of c-*myc* RNA were determined relative to total poly(A)-containing transcripts by hybridization to a poly(dT) probe rather than to specific mRNAs such as actin or

* Corresponding author.

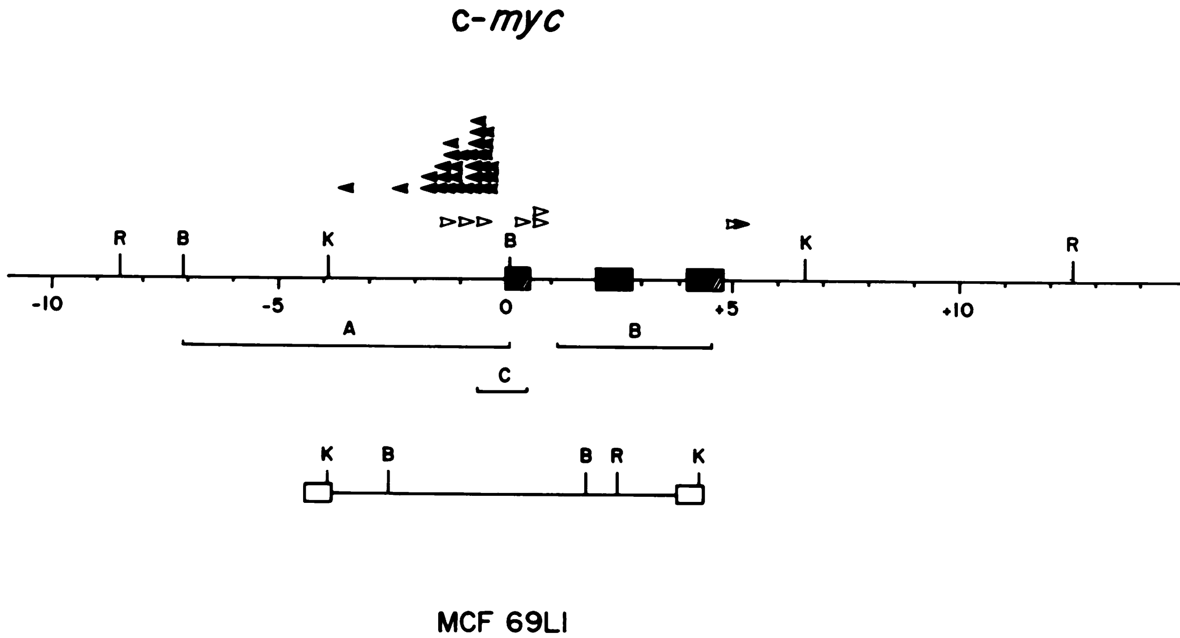

FIG. 1. DNA rearrangements at the c-*myc* locus in AKR/J thymomas owing to proviral integration. Shown are restriction maps of the c-*myc* locus and of MCF 69L1 proviral DNA obtained with endonucleases *Eco*RI (R), *Bam*HI (B), and *Kpn*I (K). Arrows show the integration sites and transcriptional orientation of MCF 69L1 proviruses determined by use of multiple restriction enzymes and multiple probes of the c-*myc* locus. Probe A, pB5'-myc (5); probe B, pα25BH3.4 (21); probe C, R*S10 (26). Scale is in kilobases.

β2-microglobulin which are used widely in such measurements. We wanted to avoid the possibility that the normalization standard might vary between normal and tumor tissue independently of c-*myc*. In fact, when slot blots were probed with actin and poly(dT) it was apparent that the actin levels in normal thymus were at least twice those of thymomas (data not shown). Thus, normalization of c-*myc* data to actin resulted in a two- to fourfold-higher estimate of c-*myc* levels in thymomas than normalization to poly(A)$^+$ RNAs.

Figure 2b and Table 1 show the relative levels of c-*myc* RNA in thymomas with or without c-*myc* DNA rearrangements compared with that in normal 2-month-old AKR mouse thymus. Values represent the average of two to four independent slot-blot determinations. The standard deviation of such measurements was approximately ±40%.

Of the thymoma RNA samples which were analyzed, 11 of 21 were derived from tumors which had proviral integrations near c-*myc*. Southern blots of these tumor DNAs showed that the rearranged DNA fragments were of germ line

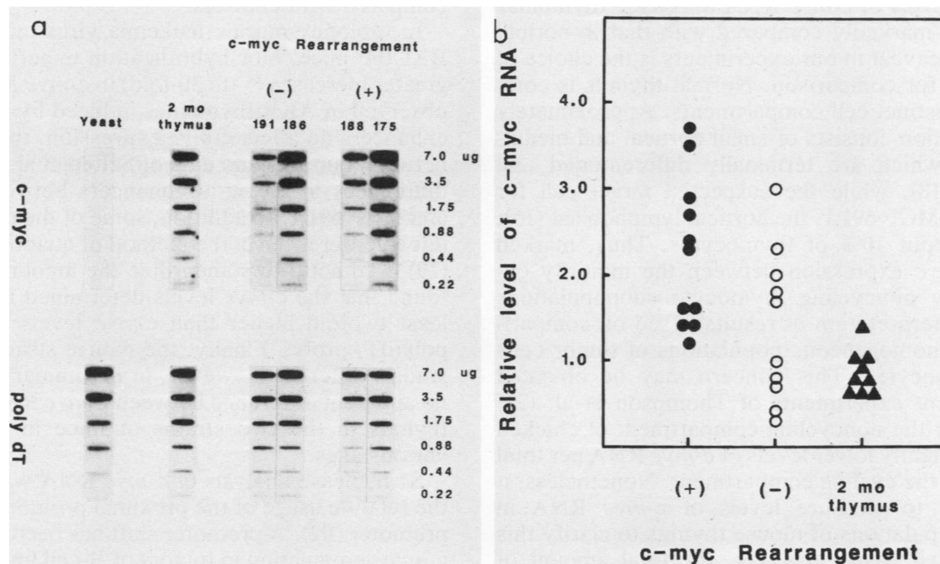

FIG. 2. Blot hybridization analysis of steady-state c-*myc* RNA in normal 2-month-old AKR/J mouse thymus and MCF 69L1-induced AKR/J thymomas with (+) or without (−) detectable c-*myc* DNA rearrangements. (a) Slot-blot analysis of c-*myc* RNA and of poly(A)-containing RNA. (b) Relative levels of c-*myc* RNA as determined by densitometric analysis of RNA slot blots and normalized to the amount of poly(A)-containing RNA added per sample as detected with the poly(dT) probe. The c-*myc* RNA level of one normal thymus sample was assigned the value of 1.0 for comparison.

intensity and demonstrated that the tumor consisted predominantly of a single clone. The c-*myc* RNA levels in these thymomas were on average three times higher than the level of c-*myc* RNA found in normal thymus and ranged from about one to four times normal. No correlation was observed between c-*myc* RNA levels and proviral integration sites. The c-*myc* RNA levels in thymomas without c-*myc* DNA rearrangements were lower on average than those in thymomas with rearrangements, but, as shown in Fig. 2b, considerable variation was observed among different tumors with values overlapping those of both normal thymus and thymomas with c-*myc* rearrangements.

The murine c-*myc* gene is normally transcribed from two initiation sites designated P1 and P2 (11, 22, 26), which are separated by 163 base pairs (1, 20). Accordingly, we assessed the relative usage of the two c-*myc* promoters in the RNA samples analyzed by slot-blot analysis by means of S1 nuclease mapping (Fig. 3). Surprisingly, the ratio of promoter usage (P1/P2) increased in virtually all thymomas tested, regardless of whether a c-*myc* rearrangement was detected. Although the two normal thymuses from 2-month-old AKR/J mice had P1/P2 ratios of 0.24 and 0.29, respectively, the upper limit of normal tissue was taken as 0.45, based on recent reports that P1/P2 ratios as high as 0.45 were observed in a variety of normal tissues (22, 26). Most of the thymomas tested (13 of 16) had P1/P2 ratios greater than 0.45. The average P1/P2 ratio of those tumors with c-*myc* rearrangements, excluding tumor 188, was 1.2. Sample 188 was the only thymoma with a c-*myc* rearrangement which did not have an altered promoter ratio in favor of P1. Interestingly, this was the only thymoma of those tested by S1 nuclease analysis which had a viral integration downstream of exon 3. The remaining eight samples with c-*myc* rearrangements had proviruses integrated in the reverse orientation and were found upstream of exon 1.

Of the samples without detectable c-*myc* rearrangements, five of seven had P1/P2 ratios greater than 0.45. The average ratio of such samples with elevated ratios was 1.0.

Blot hybridization analysis of total cellular RNA showed that steady-state levels of c-*myc* RNA in AKR/J thymomas were not elevated markedly compared with that in normal thymus tissues. A caveat in our experiments is the choice of control cells used for comparison. Normal thymus is composed of several distinct cell compartments. Approximately 85% of the population consists of small cortical and medullary thymocytes which are terminally differentiated and noncycling (17a, 18), while the suspected target cell for transformation by MCF 69L1, the cortical lymphoblast (15), makes up only about 10% of thymocytes. Thus, marked differences in c-*myc* expression between the minority cycling and majority noncycling thymocyte subpopulations could affect the interpretation of results based on comparisons of relatively homogeneous populations of tumor cells with normal thymocytes. This concern may be obviated somewhat by recent experiments of Thompson et al. (24) which showed that the noncycling compartment of chicken thymus had only slightly lower levels of c-*myc* RNA per total cellular RNA than the cycling compartment. Nonetheless, it will be important to measure levels of c-*myc* RNA in fractionated subpopulations of mouse thymus to clarify this point. On a per cell basis, however, the total amount of c-*myc* RNA in leukemic blast cells actually has increased more than indicated by the specific measurement of c-*myc* RNA relative to total mRNA because flow cytometric measurements of RNA with acridine orange staining have shown that the mean RNA content of leukemia cells is approximately twofold higher than that in normal thymocytes (14). Similar results were reported in mouse plasmacytomas in which relative c-*myc* RNA levels were only four times higher than those in quiescent B cells (7). In this latter work it was estimated that tumor cells contained eight times more RNA resulting in a 30-fold-higher level of c-*myc* RNA per cell compared with controls.

TABLE 1. Steady-state measurements of c-*myc* RNA transcripts in primary thymomas induced in AKR/J mice by MCF 69L1

Thymoma	Proviral integration site[a]	c-*myc* RNA level[b]	P1/P2[c]
117	−0.6	2.4	1.3
118	−0.5	2.3	0.70
119	NR[d]	1.0	1.0
120	NR	2.3	0.90
131	NR	1.8	1.1
134	NR	0.8	ND[e]
144	NR	1.7	0.4
157	−0.65	1.6	1.3
175	−1.25	3.7	1.6
176	NR	3.0	1.4
182	−0.35	3.5	0.6
185	−1.65	2.9	0.8
186	NR	2.0	0.3
187	+0.7	2.7	ND
188	+5.2	1.2	0.2
189	NR	0.7	0.65
191	NR	0.3	ND
E2	NR	0.4	ND
E3	−0.9	1.4	1.8
E4	−1.5	1.4	1.2
E5	−0.7	1.6	ND

[a] Proviral integration sites were determined as described in the legend to Fig. 1. Sites are expressed as kilobases relative to the 5′ terminus of exon 1.
[b] RNA levels were determined by slot-blot analysis.
[c] P1/P2, Ratio of c-*myc* RNA transcripts initiated from the proximal promoter P1 and the distal promoter P2 as determined by S1 nuclease analysis.
[d] NR, No DNA rearrangement detectable within the 21-kb *Eco*RI fragment containing the entire c-*myc* locus.
[e] ND, Not determined.

In Moloney murine leukemia virus-induced leukemias in BALB/c mice, blot hybridization experiments (19) showed greater increases (5- to 30-fold) in c-*myc* RNA levels than we observed in AKR thymomas induced by MCF 69L1. If viral enhancers do affect c-*myc* expression, then the discrepancy between our data and data of Selten et al. (19) may be due to differences in the viral enhancers between Moloney virus and MCF 69L1. In addition, some of the discrepancy may be due to differences in the method of quantitation. Selten et al. (19) used actin to standardize the amount of RNA, and we found that the c-*myc* levels determined in this way were at least twofold higher than c-*myc* levels determined with a poly(dT) probe. Finally, the mouse strains used in the two studies differed. However, in preliminary studies we found no apparent difference between c-*myc* RNA levels in normal thymus in the two strains of mice in question tested at various ages.

S1 nuclease analysis of c-*myc* RNA was used to measure the relative usage of the proximal promoter (P1) to the distal promoter (P2). A promoter shift has been viewed as a sign of c-*myc* deregulation in tumors of B-cell lineage (8, 11, 23, 26). Remarkably, all thymomas with proviral integrations upstream of exon 1 resulted in a shift in the P1/P2 ratio. It is likely that shifts in the P1/P2 ratio indicate differences in rates of transcription from the two promoters and not differential stabilities of the two mRNA species since the two

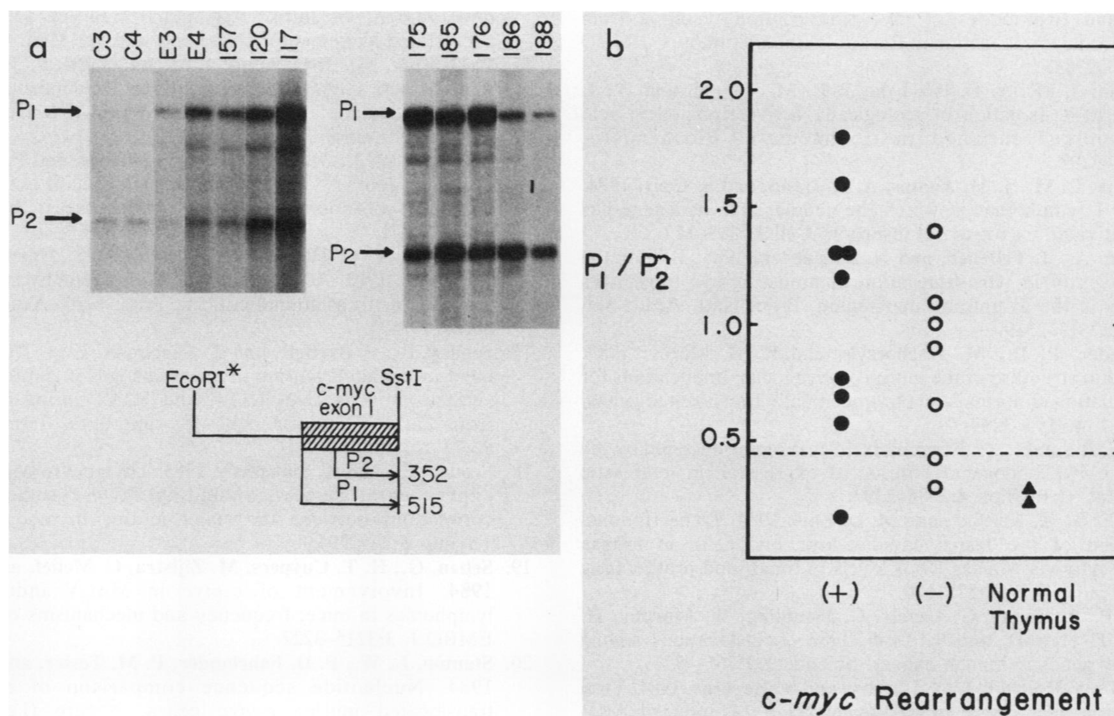

FIG. 3. S1 nuclease mapping of RNA transcripts from c-*myc* promoters P1 and P2 in normal AKR/J thymus and in AKR/J thymomas induced by MCF 69L1. (a) S1 nuclease analysis (26) of total cellular RNA (30 μg) with probe C (Fig. 1). RNA samples from normal 2-month-old AKR/J mouse thymus are represented by lanes C3 and C4. In these measurements RNA input was not normalized by independent S1 nuclease analysis of other cellular genes so strict quantitative comparisons between samples are not valid. (b) P1/P2 ratios derived from densitometeric scans of autoradiographs of S1 mapping. Dotted line represents upper limit of normal P1/P2 ratio as determined from S1 analysis of numerous normal tissues (22, 26). On the abscissa are indicated thymomas with (+) or without (−) detectable proviral integrations near c-*myc*.

transcripts appear to have comparable stabilities in different cell types (6, 15a). The promoter shift may reflect viral enhancer activity causing an increase in transcription with, perhaps, a preferential effect on the promoter closest to it (P1). Alternatively, there may be a regulatory element within the region upstream of exon 1 whose function is to downregulate both P1 and P2. Viral integration in the region might destroy the element resulting in the increased levels of c-*myc* transcripts.

We also found evidence for c-*myc* deregulation in cases in which viral integrations were not detectable in the 21-kb c-*myc* fragment analyzed. Seven thymomas in this category were analyzed by S1 nuclease analysis, and five showed a promoter shift. These samples may contain viral integrations outside the 21-kb area scanned, and the virus may be exerting its influence via a long-range *cis*-acting mechanism. Or, there may be point mutations in the c-*myc* locus which affect transcription. Lastly, the virus may have integrated near a gene which regulates expression of c-*myc* such as a *trans*-acting repressor suggested by Leder and co-workers (8). If such a gene interacted with the c-*myc* locus to depress P1 expression, a viral integration event which disrupted or altered the regulation of this gene might result in the P1 shift detected.

Promoter shifts seen in thymomas without detectable c-*myc* rearrangements indicate that c-*myc* deregulation may be implicated in virtually all the MCF 69L1-induced thymomas and may be a general mechanism in T-cell leukemogenesis. This finding points to a mechanism, aside from viral integration within the immediate vicinity of the c-*myc* gene, which results in an altered control of *myc* expression.

It remains to be determined how the altered balance of c-*myc* transcripts found in B- and T-cell malignancies affects cellular physiology. Abnormal *myc* promoter usage could be manifested in a temporal change in *myc* gene expression which could alter normal growth control. A recent study of the c-*myc* proteins speculated that the two different messages were translated into two different proteins, possibly with different functions (6). In another study it was proposed that the size of transcripts and resulting secondary structure may affect translational efficiency (17). Thus, a shift in the P1/P2 ratio could conceivably lead to increased expression of the c-*myc* protein. However, two recent studies which measured c-*myc* translational efficiency have produced conflicting results as to the role of exon 1 sequences in translational control (4, 12). Alternatively, the c-*myc* RNA transcripts themselves could serve some function. Further work will be necessary to answer this crucial issue.

This work was supported by Public Health Service grants CA 31491, CA 36246, and CA 16599 from the National Cancer Institute. K.B.M. is a Research Career Development Awardee of the National Institute of Allergy and Infectious Diseases.

We would like to thank J. Teumer and E. Stavnezer for suggesting the poly(dT) method of standardizing poly(A)-containing RNA and for giving us their assay protocols and Paul Fahrlander for the pB5′-myc probe.

LITERATURE CITED

1. **Bernard, O., S. Cory, S. Gerondali, E. Webb, and J. M. Adams.** 1983. Sequence of the murine and human cellular myc onco-

genes and two modes of myc transcription resulting from chromosome translocation in Burkitt lymphoid tumours. EMBO J 2:2375–2383.

2. **Chirgwin, J. M., A. E. Przybyla, J. R. Macdonald, and W. J. Rutter.** 1979. Isolation of biologically active ribonucleic acid from sources enriched in ribonuclease. Biochemistry **18:**5294–5299.
3. **Corcoran, L. M., J. M. Adams, A. R. Dunn, and S. Cory.** 1984. Murine T lymphomas in which the cellular *myc* oncogene has been activated by retroviral insertion. Cell **37:**113–122.
4. **Darveau, A., J. Pelletier, and N. Sonenberg.** 1985. Differential efficiencies of *in vitro*-translation of mouse c-*myc* transcripts differing in the 5′ untranslated region. Proc. Natl. Acad. Sci. USA **82:**2315–2319.
5. **Fahrlander, P. D., M. Piechaczyk, and K. B. Marcu.** 1985. Chromatin structure of the murine c-*myc* locus: implications for the regulation of normal and chromosomally translocated genes. EMBO J. **4:**3195–3202.
6. **Hann, S. R., and R. N. Eisenman.** 1984. Proteins encoded by the human c-*myc* oncogene: differential expression in neoplastic cells. Mol. Cell. Biol. **4:**2486–2497.
7. **Keath, E. S., A. Kelekar, and M. D. Cole.** 1984. Transcriptional activation of the translocated c-*myc* oncogene in mouse plastmacytomas: similar RNA levels in tumor and proliferating normal cells. Cell **37:**521–528.
8. **Leder, P., J. Battey, G. Lenoir, C. Moulding, W. Murphy, H. Potter, T. Stewart, and R. Taub.** 1983. Translocations among antibody genes in human cancer. Science **222:**765–777.
9. **Li, Y., C. A. Holland, J. W. Hartley, and N. Hopkins.** 1984. Viral integration near c-*myc* in 10-20% of MCF 247-induced AKR lymphomas. Proc. Natl. Acad. Sci. USA **81:**6808–6811.
10. **Maniatis, T., E. F. Fritsch, and J. Sambrook.** 1984. Molecular cloning, a laboratory manual. Cold Spring Harbor Laboratory, Cold Spring Harbor, N.Y.
11. **Marcu, K. B., J. Q. Yang, L. W. Stanton, J. F. Mushinski, P. D. Fahrlander, L. A. Eckhardt, and B. K. Birshtein.** 1984. Activation of the c-*myc* oncogene in murine plasmacytomas, p. 11–27. *In* B. Wahren, G. Holm, S. Hammerstrom, and P. Perlman (ed.), Molecular biology of tumor cells, progress in cancer research and therapy. Raven Press, New York.
12. **Nilsen, T. W., and P. A. Maroney.** 1984. Translational efficiency of c-myc mRNA in Burkitt lymphoma cells. Mol. Cell. Biol. **4:**2235–2238.
13. **O'Donnell, P. V., E. Fleissner, H. Lonial, C. Koehne, and A. Reicin.** 1985. Early clonality and high-frequency proviral integration into the c-*myc* locus in AKR leukemia. J. Virol. **55:**500–503.
14. **O'Donnell, P. V., and F. Traganos.** 1985. Changes in thymocyte proliferation at different stages of viral leukemogenesis in AKR mice. J. Immunol. **136:**720–727.
15. **O'Donnell, P. V., R. Woller, and A. Chu.** 1984. Stages in development of mink cell focus inducing (MCF) virus-accelerated leukemia in AKR mice. J. Exp. Med. **160:**914–934.

15a. **Piechaczyk, M., J.-Q. Yang, J. M. Banchard, P. Jeanteur, and K. B. Marcu.** 1985. Post-transcriptional mechanisms are responsible for accumulation of truncated c-*myc* RNAs in murine plasma cell tumors. Cell **42:**589–597.

16. **Rigby, P. W. J., M. Dieckmann, C. Rhodes, and P. Berg.** 1977. Labelling deoxyribonucleic acid at high specific activity in vitro by nick translation with DNA polymerase I. J. Mol. Biol. **133:**237–251.
17. **Saito, H., A. C. Hayday, K. Wiman, W. S. Hayward, and S. Tonegawa.** 1983. Activation of the c-*myc* gene by translocation: a model for translational control. Proc. Natl. Acad. Sci. USA **80:**7476–7480.

17a. **Scollay, R., P. Bartlett, and K. Shortman.** 1985. T cell development in the adult murine thymus: changes in expression of the surface antigens Ly2, L3T4, and B2A2 during development from early precursor cells to emigrants. Immunol. Rev. **82:**79–103.

18. **Scollay, R., and K. Shortman.** 1983. Thymocyte populations: an experimental review, including flow cytometric cross-correlations between the major murine thymocyte markers. Thymus **5:**245–295.
19. **Selten, G., H. T. Cuypers, M. Zijlstra, C. Melief, and A. Berns.** 1984. Involvement of c-*myc* in MuLV induced T-cell lymphomas in mice: frequency and mechanisms of activation. EMBO J. **3:**3215–3222.
20. **Stanton, L. W., P. D. Fahrlander, P. M. Tesser, and K. Marcu.** 1984. Nucleotide sequence comparison of normal and translocated murine c-*myc* genes. Nature (London) **310:**423–425.
21. **Stanton, L. W., R. Watt, and K. B. Marcu.** 1983. Translocation, breakage and truncated transcripts of c-myc oncogene in murine plasmacytomas. Nature (London) **303:**401–406.
22. **Stewart, T. A., A. R. Bellve, and P. Leder.** 1984. Transcription and promoter usage of the c-*myc* gene in normal somatic and spermatogenic cells. Science **226:**707–710.
23. **Taub, R., C. Moulding, J. Battey, W. Murphy, T. Vasicek, G. M. Lenoir, and P. Leder.** 1984. Activation of somatic mutation of the translocated c-myc gene in Burkitt lymphoma cells. Cell **36:**339–348.
24. **Thompson, C. B., P. B. Challoner, P. E. Neiman, and M. Groudine.** 1985. Levels of c-*myc* oncogene mRNA are invariant throughout the cell cycle. Nature (London) **314:**363–366.
25. **Weiss, R., N. Teich, H. Varmus, and J. Coffin.** 1985. Molecular biology of tumor viruses, 2nd ed., supplements and appendices. Cold Spring Harbor Laboratory, Cold Spring Harbor, N.Y.
26. **Yang, J. Q., S. R. Bauer, J. F. Mushinski, and K. B. Marcu.** 1985. Chromosome translocations clustered 5′ of the murine c-*myc* gene qualitatively affect promoter usage: implications for the site of normal c-*myc* regulation. EMBO J **4:**1441–1447.